# Enhanced Effects of Lithocholic Acid Incorporation into Liquid Crystalline Biopolymer Poly(Coumaric Acid) on Structural Ordering and Cell Adhesion

*Michiya Matsusaki,*[1] *Tran Hang Thi,*[1,2] *Tatsuo Kaneko*[1] *and Mitsuru Akashi*[1,*]

[1]Department of Molecular Chemistry, Graduate School of Engineering, Osaka University, 2-1 Yamada-oka, Suita 565-0871, Japan

[2]Department of Nanostructured and Advanced Materials, Graduate School of Science and Engineering, Kagoshima University, 1-21-40 Korimoto, Kagoshima 890-0065, Japan

[*]Author to whom correspondence should be addressed.

Mitsuru Akashi, Professor

Tel +81-6-6879-7356

Fax +81-6-6879-7359

E-mail: akashi@chem.eng.osaka-u.ac.jp

**ABSTRACT.** A novel thermotropic liquid crystalline biocopolymer, poly{4-hydroxycinnamic acid (4HCA: coumaric acid)-co-lithocholic acid (LCA)}, was synthesized by a thermal polycondensation of 4HCA and LCA. When the LCA molar composition of P(4HCA-*co*-LCA)) was 0, 5, 7, 23, 27, and 45 mol%, the copolymers showed a nematic liquid-crystalline phase. The melting point of the copolymers was 120-250 $^{o}$C depending on the LCA composition, and showed a maximum at 7 mol%. Wide angle X-ray diffraction (WAXD) analysis showed a typical diffraction pattern of a hexagonal arrangement for 0, 7, 23, and 27 mol% LCA molar composition, which were cooled from a nematic melt. The other polymers showed no distinct diffraction. In particular, the copolymer of 7 mol% LCA molar composition showed four distinct diffractions corresponding to spacings with a reciprocal ratio of 1, $3^{0.5}$, 2, and $7^{0.5}$, indicating the highest structural ordering of all copolymers prepared here. The results of the cell adhesion and static contact angle tests suggest that the 7 mol% LCA molar composition copolymer had the highest hydrophobicity and cell adhesion ability, which was easily controlled by altering in feed. We conclude that the structural ordering may have a significant correlation with cell adhesion activity.

## Introduction

Liquid-crystalline polymers have been used in several fields[1-6] because the molecular arrangement can be regulated by altering the temperature,[7-9] concentration,[10] electric field, magnetic field, and other factors[11-17]. On the other hand, thermotropic synthetic liquid-crystalline polymers have rarely been used in the biological and medical fields, because biocompatibility and biodegradability are strictly required for biomedical applications. The liquid-crystalline properties of several natural biopolymers such as DNA,[18-20] RNA,[21] hemoglobin S (HbS),[22] F-actin[23] and polysaccharides[24,25] have been reported. However, their applications in biological devices are limited because of poor availability, low stability and low processability. In order to solve these restrictions, it is expected that a mesogenic "biomonomer", whose homopolymer shows a liquid-crystalline nature, can extend the variety of molecular designs for liquid-crystalline biopolymers.

We have already reported the polymerization of *trans*-4-hydroxycinnamic acid (4HCA: coumaric acid) as a "biomonomer" and investigated its liquid-crystalline behavior, photoreactivity and cell compatibility.[26,27] 4HCA exists in plant cell walls as an intermediate metabolite of lignin and other biological materials,[28] and shows [2+2] cycloaddition and *trans/cis* isomerization. The 4HCA homopolymer (P4HCA) formed a crystalline structure with hexagonal chain packing below 215 $^{o}$C, and a nematic liquid-crystalline structure at 215–280 $^{o}$C. P4HCA showed a photoreaction in its liquid-crystalline state, and had cell compatibility. It is expected that P4HCA can be applied to biomedical and environmental materials.

In this study, we report the synthesis and evaluation of the copolymer poly{4HCA-co-lithocholic acid (LCA)} (P(4HCA-*co*-LCA)). LCA exists in mammalian bile as a cholesteric derivative, and is expected to show good biocompatibility and high structural rigidity based on its steroid skeleton. The copolymers are expected to have the characteristics of LCA, such as control in solubility, processability, melting point ($T_m$), and the cell adhesion properties of P4HCA while keeping the liquid-crystalline property of

P4HCA. We report here the relationship between the structural ordering and the cell adhesion of P(4HCA-*co*-LCA).

## Materials and Methods

**Materials.** 4HCA and LCA used as monomers were purchased from Tokyo Kasei (Tokyo, Japan), and were used as received. Pentafluorophenol used as a casting solvent was purchased from Tokyo Kasei (Tokyo, Japan), and was used as received. Acetic anhydride and sodium acetate were used for polymerization and were purchased from Wako Pure Chemical Industries (Osaka, Japan), and were used without further purification. Pentafluorophenol-*d* used as the NMR solvent was purchased from SIGMA-Aldrich (Missouri, USA), and was used as received. Other chemicals were purchased from Nacalai Tesque (Kyoto, Japan) and were used without further purification.

**Synthesis of P(4HCA-*co*-LCA).** P(4HCA-*co*-LCA) was obtained by thermal polycondensation according to previous studies with minor modifications (Scheme 1).[26,27] 4HCA (10 mmol) and LCA (2.5 mmol) were stirred at 200$^{o}$C for 6 hours in the presence of 10 mL acetic anhydride as a condensation reagent, and sodium acetate (trace) as a catalyst for the transesterfication. The molten mixture gradually became more viscous upon increasing the reaction time. After the reaction, the product was dissolved in pentafluorophenol and purified by reprecipitation over ethanol twice, and was washed with ethanol by a Soxhlet extraction method for 36 hours. The yield was 52 % (average value of three times). The average molecular weight of P(4HCA-*co*-LCA) was determined in tetrahydrofuran (THF) by a GPC (Shimadzu LC-6A system with a TSK-GEL Super H2000 column), calibrated with polystyrene standards at a flow rate of 0.6 ml/min, 40$^{o}$C.

**Observation of thermotropic properties by crossed-polarizing microscopy.** The phase transition of P(4HCA-*co*-LCA) was observed by crossed-polarizing microscopy. The samples were sandwiched between two glass plates, and were heated at a rate of 10 $^{o}$C/min by a METTLER TOLEDO FP82HT Hot Stage (Greifensee, Switzerland). The $T_m$ and the liquid-crystalline phase were observed directly by

microscopy, and were also confirmed by differential scanning calorimetry (DSC) measurement (EXSTAR6100; Seiko Instruments Inc., Chiba, Japan).

**Structural analysis of P(4HCA-*co*-LCA).** The relationship between the molecular orientation of P(4HCA-*co*-LCA) and the LCA molar ratio was analyzed by wide angle X-ray diffraction (WAXD) with a Geigerflex RAD-IIB (Rigaku Co., Tokyo, Japan) at scanning angles that ranged from 50° to 10° at 2° $min^{-1}$. The copolymers were cooled from their $T_m$ before the WAXD measurement.

**Cell adhesion property.** P(4HCA-*co*-LCA) disks were prepared in order to perform the cell adhesion test. A total of 40 mg of sample plus 10 μl distilled water were added into a compressor holder, and compressed under vacuum at 300 $kg/cm^2$ for 5 min. After molding, the disks (1 cm diameter and 0.4 mm height) were vacuum dried for 24 hours at room temperature. We performed a L929 fibroblast cell adhesion test using these disks. Various disks were fixed onto 24-well multiplates by a stainless ring, and L929 cells were seeded onto the disks at 10 x $10^4$ cells/well. The cells were incubated for 24 hours at 37°C in Eagle's minimal essential medium (MEM) containing 10% FCS, and were washed twice with phosphate buffered saline. The number of cells adhered onto the disks was counted with trypan blue staining on a hemocytometer.

**Static contact angle measurement of spin-coated films.** The static contact angle of spin-coated P(4HCA-*co*-LCA) films was investigated in order to characterize their surface. The copolymers were dissolved in pentafluorophenol at 1 wt%, and 100 μl aliquots were dropped onto glass plates. After spin coating at 2000 rpm for 90 seconds, the spin-coated films were dried *in vacuo* for 24 hours at 50°C. We measured the static contact angle of the spin-coated films by the sessile drop method with a goniometer type G-1 (Erama Co., Tokyo, Japan) and distilled water at room temperature. The volume of the water in the drop was 3 μL. All reported values represent the average of six measurements taken at different locations on the film surface.

## Results and Discussion

**Synthesis of P(4HCA-*co*-LCA)**. LCA has a very stiff steroid plane with a hydroxyl group perpendicular to the plane, and a flexible short aliphatic chain with a carboxyl end group. The effects of this unique structure on the structure and properties of P(4HCA-*co*-LCA)s were investigated. Table 1 shows the synthetic conditions and copolymer composition of P(4HCA-*co*-LCA)s. The monomers were dissolved at 140°C. The solution was transparent initially, however when the temperature was increased to 170-180°C, the solution changed to an ocher color and began to show increased viscosity. After 15-20 min, the reaction solution changed to a melting compound. The purified products were obtained as an ocher powder which was soluble in pentafluorophenol and trifluoroacetic acid (TFA)/dichloromethane (DCM) (1/5 v/v%), but when the LCA molar ratio was 45 mol% or higher, the copolymers were dissolved in alcohols, acetone, acetonitrile, THF, chloroform and aprotic amidic solvents (Table 2). We previously reported that a higher molar composition of D,L-lactic acid (DLLA) in poly(4HCA-co-DLLA) gave a better solubility in organic solvents, presumably due to the reduced chain rigidity.[26] LCA may also have reduced chain rigidity, in other words, the flexible chain and the hydroxyl perpendicular alignment for LCA may create an elbow for the polymeric chain. The LCA molar compositions in the copolymers were lower than those in the feed, and the yields decreased with increasing LCA composition in the feed. These results are due to lower chemical reactivity of LCA because of steric hindrance by the bulky steroid plane around the hydroxyl group.

Figure 1 shows FT/IR spectra of the monomers and copolymers. The IR peaks assigned to the double bond group ($\nu_{C=C}$: 1626, 1633 and 1634 $cm^{-1}$) and aromatic group ($\nu_{p=\phi}$: 1599 and 1600 $cm^{-1}$) in the spectrum for the 4HCA monomer appeared in those for P4HCA and P(4HCA-*co*-LCA). On the other hand, the IR peaks assigned to the carboxyl groups in the spectra for the LCA ($\nu_{C=O}$: 1701 $cm^{-1}$) and 4HCA ($\nu_{C=O}$: 1668 $cm^{-1}$) monomers disappeared in both the homopolymer and the copolymer. Instead, the IR peaks assigned to the ester groups ($\nu_{C=O}$: 1730, 1732 and 1733 $cm^{-1}$) appeared, indicating the successful conversion of the carboxylic acids to esters. The shoulder peaks of P(4HCA-*co*-LCA) and P4HCA (1689 $cm^{-1}$) would be assigned to the terminal carboxyl groups. Figure 2 shows the $^{1}$H-NMR

spectrum of P(4HCA-*co*-LCA-77/23) in TFA-*d*/DCM-*d* (1/5 v/v%). Multiple peaks in the region of the chemical shift (δ = 6.54-8.09 ppm) were assigned to aromatic protons (a), and a single peak at δ = 4.95 ppm was assigned to the steroid end proton present nearest to the hydroxyl moiety (b). The molar composition of LCA in the copolymers were calculated by the peak area ratios of (a) and (b). The average molecular weight of P(4HCA-*co*-LCA) was measured in THF by GPC. P(4HCA-*co*-LCA)s with LCA compositions of 45, 65, and 100 mol% showed a GPC single peak, indicating a successful copolymerization. While a polydispersity (*Mw/Mn*) was 1.46, 1.64 and 1.51, the weight-average oligomeric molecular weight *Mw* was 3370, 2700 and 1280, respectively. The molecular weight decreased with increasing LCA content, presumably due to the low chemical reactivity of LCA. Although we could not measure the molecular weight of the other copolymers with higher LCA compositions because of their low solubility, we can expect a higher molecular weight and successful copolymerization. The observation of the highly viscous molten liquid typical of the polymeric samples as well as the results of the FT/IR, $^{1}$H-NMR, solubility test and GPC indicated that P(4HCA-*co*-LCA) was successfully synthesized by thermal polycondensation.

**Thermotropic properties of P(4HCA-*co*-LCA)**. The thermotropic properties were investigated by crossed-polarizing microscopic observation and DSC measurement. The results of the microscopic observation showed almost the same results as the DSC analysis. The glass transition temperatures of the copolymers, $T_g$, ranged between 160-170$^{o}$C independent of the LCA composition. The relationship between the LCA molar composition and $T_m$ is shown in Figure 3. P4HCA showed a $T_m$ at 220$^{o}$C as shown in a previous report.[27] In the copolymers, the $T_m$ increased with increasing LCA molar composition until 7 mol%, and showed its highest value at 250 °C. Above 7 mol%, the $T_m$ decreased. In the case of LCA compositions over 45 mol%, P(4HCA-*co*-LCA) and PLCA showed no $T_m$, suggesting that they were amorphous polymers. Crossed-polarizing microscopy showed that P(4HCA-*co*-LCA) with LCA compositions of 45 mol% and lower showed strong birefringence above the $T_m$, and sometimes a banded texture as shown in the representative photograph taken under the conditions

marked by the closed circle (inset of Figure 3). The texture was easily transformed into another morphology, including the dark-field view by sliding the coverglass. These results indicated that P(4HCA-*co*-LCA)s with LCA composition of 45 mol% and lower exhibited a nematic phase, where the polymer chains were autonomously oriented but randomly located. All of the nematic liquids solidified at 300 °C upon subsequent heating, and no longer appeared with successive heating and cooling cycles. It became pale yellow in color and an insoluble solid in pentafluorophenol and other solvents. The same phenomenon was observed for P4HCA,[27] suggesting that this crystallization was based on the chemical conversion of the 4HCA units, such as decomposition. As a whole, the phase diagram in Figure 3 showed that the melting point of the copolymers can be controlled while retaining the liquid-crystalline properties. In addition, one can see that the high percentage of LCA in the composition resulted in a liquid crystalline copolymer, although PLCA is not a liquid crystalline polymer itself. On the other hand, P(4HCA-co-DLLA) copolymers, which were previously prepared,[26] exhibited a nematic phase at a DLLA molar composition below 30 mol%, but other copolymers did not show a liquid crystalline phase. LCA has a greater ability to maintain the liquid crystalline state of the copolymer comprised of 4HCA and itself than DLLA, which may be associated more with higher structural rigidity of LCA than DLLA. Unexpectedly, P(4HCA-co-DLLA) or P(4HCA-co-LCA) showed no chiral liquid crystalline phase such as a cholesteric phase.

**Structural analysis of P(4HCA-*co*-LCA).** The unique melting property of P(4HCA-*co*-LCA)s may be associated with its structure. WAXD studies of P(4HCA-*co*-LCA)s, which was cooled from a nematic melt, were performed (Figure 4a). The WAXD pattern of P4HCA showed four distinct diffractions at $2\theta$ = 10.3 (d1), 17.6 (d2), 23.0 (d4) and 26.8$^{o}$ (d5) ($\theta$: diffraction angle), corresponding to spacings of 0.86, 0.50, 0.39 and 0.33 nm, respectively. As discussed in the previous paper, P4HCA was highly crystallized, and the diffractions of d1, d2, and d5 were assigned to the hexagonal arrangement and the spacing of d4 approximates to one half of the length (0.40 nm) of the 4HCA unit. Unexpectedly, however, the satellite diffraction of d1 was absent. In the copolymer with a LCA

composition of 7 mol%, the diffraction of d3 appeared at $2\theta$ = 20.5, corresponding to a spacing of 0.43 nm, and thus can be regarded as a second-order diffraction of d1. The appearance of d3 supports a hexagonal arrangement of the polymer chains; the reciprocal spacings of diffractions of d1, d2, d3 and d5 for the copolymer with a LCA composition of 7 mo% were 0.12, 0.20, 0.23 and 0.35 $nm^{-1}$, respectively, with an approximate relation of 1:root 3:2:root 7. It is also notable that d5 located at the widest diffraction angle became more intense despite the broader peaks for all diffractions. One can see that the changing behavior in peak intensity with increasing LCA composition was dependent on the type of diffraction. Therefore, we calculated the sharpness of the peaks, i.e. the ratio of the peak intensity to the full width of the half maximum, and plotted them against the LCA composition (Figure 4b). The sharpness of the main peaks of d2 and d4 decreased with increasing LCA composition, clearly indicating a decrease in the degree of crystallization. In contrast, the sharpness of the relatively small peaks of d3 and d5 increased with increasing LCA composition, which implies an enhancement of the correlation length of the hexagonal arrangement. The small number of LCA units causing structural disorder can interfere with the hexagonal arrangement, causing mismatching to occur at the crystalline domain boundary it crystallizes from the liquid crystalline state. This speculation seems to be unusual, but the enhanced effects of an amorphous structure on structural regularity have sometimes been reported. The degree of crystallization can reduce the $T_m$, while the correlation length enhancement can increase the $T_m$. These opposite effects may result in the maximum appearance of $T_m$ at an appropriate LCA composition. The diffraction peaks disappeared beyond LCA compositions of 45 mol%, indicating the amorphous effects of LCA resulted in too many elbows.

**Cell adhesion property.** In order to be useful in biological and medical devices, the cell adhesion properties of P(4HCA-*co*-LCA)s were evaluated. P(4HCA-*co*-LCA) disks were fixed into 24-well multiplates, and 10 x $10^4$ L929 cells were seeded and incubated onto the disks for 24 hours at 37 °C. Figure 5 shows the relationship between the number of adhered cells and the LCA molar composition. L929 cells adhered and extended onto these disks, and their numbers increased with increasing LCA

molar composition. In general, cell-initial adhesion is influenced by the electrical charge, roughness, hydrophilicity-hydrophobicity balance and hardness-softness balance of the surface.[29] In order to clarify the reason for the relationship between the LCA molar composition and the number of adhered cells, the static contact angles on the air side of a spin-coated film surface was measured by the sessile drop method with distilled water at 25 °C. The contact angle of P(4HCA-*co*-LCA-100/0) was 64.5±7.8°, and it increased with increasing LCA composition until 7 mol% (84.8 ± 4.9°). When the LCA composition increased above 7 mol%, the contact angle decreased gradually to 81.1 ± 1.7°. The correlation between the contact angle and the LCA molar ratio was similar to the relationship between the number of adhered cells and the LCA content. Cells are known to adhere more easily onto hydrophobic surfaces than onto hydrophilic surfaces. In addition, the surface roughness of spin-coated films did not seem to affect cell adhesion, because the roughness of all films was almost the same, and was shown to be on a nano-meter scale by atomic force microscopy (*Ra* = 3-5 nm; data not shown). Surprisingly, this cell adhesion behavior showed a good agreement with the structural and melting properties of the copolymers. The reason for the highest hydrophobicity of P(4HCA-*co*-LCA) with a LCA composition of 7 mol% may be due to the film surface structure giving the highest Tm. Although the relationship between cell compatibility and the crystallinity of the substrate thus far seems to be negligible, it will be rather important for the development of new bioactive materials.

## Conclusion

4HCA-LCA copolymers were synthesized by thermal polycondensation in the presence of anhydride acetic acid and a transesterification catalyst. When the LCA molar ratio of P(4HCA-*co*-LCA) ranged from 0 to 45 mol%, the copolymers had a nematic liquid-crystalline phase. P(4HCA-*co*-LCA-93/7) formed a crystalline structure with a hexagonal chain packing below 250 °C. Furthermore, spin-coated films of this copolymer showed high cell adhesion properties caused by its high molecular hexagonal orientation. It is expected that P(4HCA-*co*-LCA) may be useful for applications as biomedical and environmental materials. The authors are currently continuing the study of the degradability of

P(4HCA-*co*-LCA), and the synthesis of environmental plastic by 4HCA derivatives will be reported in a following paper.

**Acknowledgments.** This research was supported in part by a Grant-in-Aid from *NEDO*. We acknowledge Mr. N. Kuriyama (TOYODA GOSEI CO. LTD., Nagoya) for useful discussions.

**References and Notes.**

1. Scheffer, T. J.; Nehring, J. *Appl. Phys. Lett.* 1984, *45*, 1021.
2. Shibaev, V. P.; Kostromin, S. G.; Plate, N. A.; Ivanov, S. A.; Yu, V.; Vetrov, I.; Yakovlev, A. *Polym. Commun.* 1983, *24*, 364.
3. Meyer, R. B. *J. Phys. (France)* 1975, *36*, L69.
4. Broer, D.; Lub, J.; Mol, G. N. *Nature*, 1995, *378*, 467.
5. Hikmet, R. A. M.; Keperman, H. *Nature*, 1998, *392*, 476.
6. Kikmet, R. A. M.; Lub, J. *Prog. Polym. Sci.* 1996, *21*, 1165.
7. Demus, D. *Handbook of Liquid Crystals* (Eds Goodby, J., Gray, G. W., Spiess, H.-W. & Vill, V.) Wiley-VCH, Weinheim etc., 1998.
8. Collings, P. J.; Hird, M. *Introduction to liquid crystals* Tayor & Francis, London and Philadelphia, 1997.
9. Chandroasekhar, *S. liquid crystals (second edition)* Cambridge Univ. Press, Cambridge, 1992.
10. Brown, G. H. *Adv, Polym. Sci.* 1975, *1*, 1.
11. Yim, K. S.; Fuller, G. G.; Datko, A.; Eisenbach, C. D. *Macromolecules* 2001, *34*, 6972.
12. Pujolle-Robic, C.; Noirez, L. *Nature* 2001, *409*, 167.

13. Yamaoka, K.; Kaneko, T.; Gong, J. P.; Osada, Y. *Macromolecules*, submitted.

14. Ignés-mullol, J.; Schwartz, A. K. *Nature*, 2001, *410*, 348.

15. Kawanishi,Y.; Tamaki, T.; Seki, T.; Sakuragi, M.; Suzuki, Y.; Ichimura, K.; Aoki, K. *Langmuir* 1991, *7*, 1314.

16. Lansac, Y.; Glaser, M. A.; Clark, N. A.; Lavrentovich, O. D. *Nature*, 1999, *398*, 54.

17. Ichimura, K.; Oh, S. –K.; Nakagawa, M. *Science* 2000, *288*, 1624.

18. Robinson, C. *Tetrahedron* 1961, *13*, 219.

19. Robinson, C. *Mol. Cryst.* 1966, *1*, 467.

20. Livolant, F. *J. Phys. France* 1989, *50*, 1729.

21. Spencer, M.; Fuller, W.; Wilkins, M. H. F ; Brown, G. L. *Nature* 1962, *194*, 1014.

22. Perutz, M. F.; Liquori, A. M.; Eirich, F. *Nature* 1951, *167*, 929.

23. Coppin, C. M.; Leavis, P. C. *Biophys. J.* 1992, *63*, 794.

24. Giraud-Guille, M. *Int. Rev. Cytology* 1996, *166*, 59.

25. Suto, S.; Umeda, T. *Angew. Makromol. Chem.* 1999, *264*, 60.

26. Matsusaki, M.; Kishida, A.; Stainton, N.; Ansell, C. G. W.; Akashi M. *J. Appl. Polym. Sci.* 2001, *82*, 2357.

27. Kaneko, T.; Matsusaki, M.; Hang, T. T.; Akashi, M. *Macromol. Rapid Commun*. 2004, *25*, 673.

28. Hernanz, D.; Nunez, V.; Sancho, A. I.; Faulds, C. B.; Williamson, G.; Bartolome, B.; Gomez-Cordoves, C. *J. Agric. Food Chem*. 2001, *49*, 4884.

29. Tamada, Y.; Ikada, *Polymers in medicine II. New York and London: Plenum Publishing Corp*, 1986, p101-15.

**Figure Captions**

**Scheme 1.** Synthesis of P(4HCA-*co*-LCA).

**Table 1.** Synthesis conditions of P(4HCA-*co*-LCA).

**Table 2.** Solubility of the monomers and copolymers.

**Figure 1.** FT-IR spectra of the monomers and polymers.

**Figure 2.** $^{1}$H-NMR spectrum of P(4HCA-*co*-LCA-50/50) in TFA-*d*/DCM-*d* (1/5 v/v%).

**Figure 3.** Correlation between the LCA molar ratio and the $T_m$ of P(4HCA-*co*-LCA). The inset picture is a crossed-polarizing photomicrograph of P(4HCA-*co*-LCA-77/23) at 250 $^{o}$C.

**Figure 4.** WAXD diagrams of various LCA molar ratios of P(4HCA-*co*-LCA) recorded at 25 $^{o}$C. The samples were cooled from the liquid crystalline state.

**Figure 5.** Relationship between the LCA molar ratio of P(4HCA-*co*-LCA) and cell adhesion properties (n=3). *Statistically significant difference ($p < 0.01$) using a two-sample *t* test for each comparison. NS = no significant difference.

**Figure 6.** Relationship between the LCA molar ratio of P(4HCA-*co*-LCA) and the static contact angle (n=3).

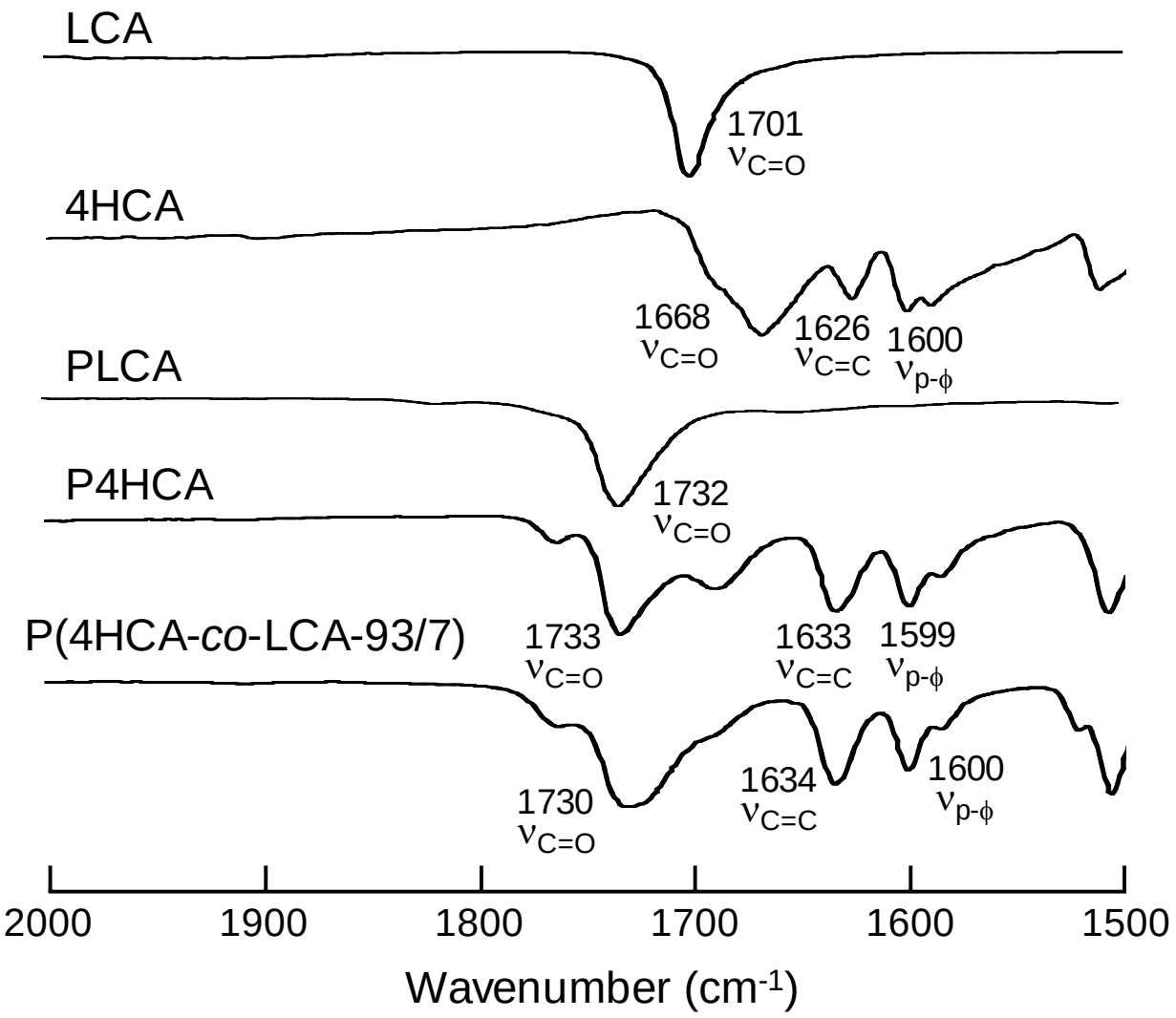


**Figure 1** Matsusaki et al.

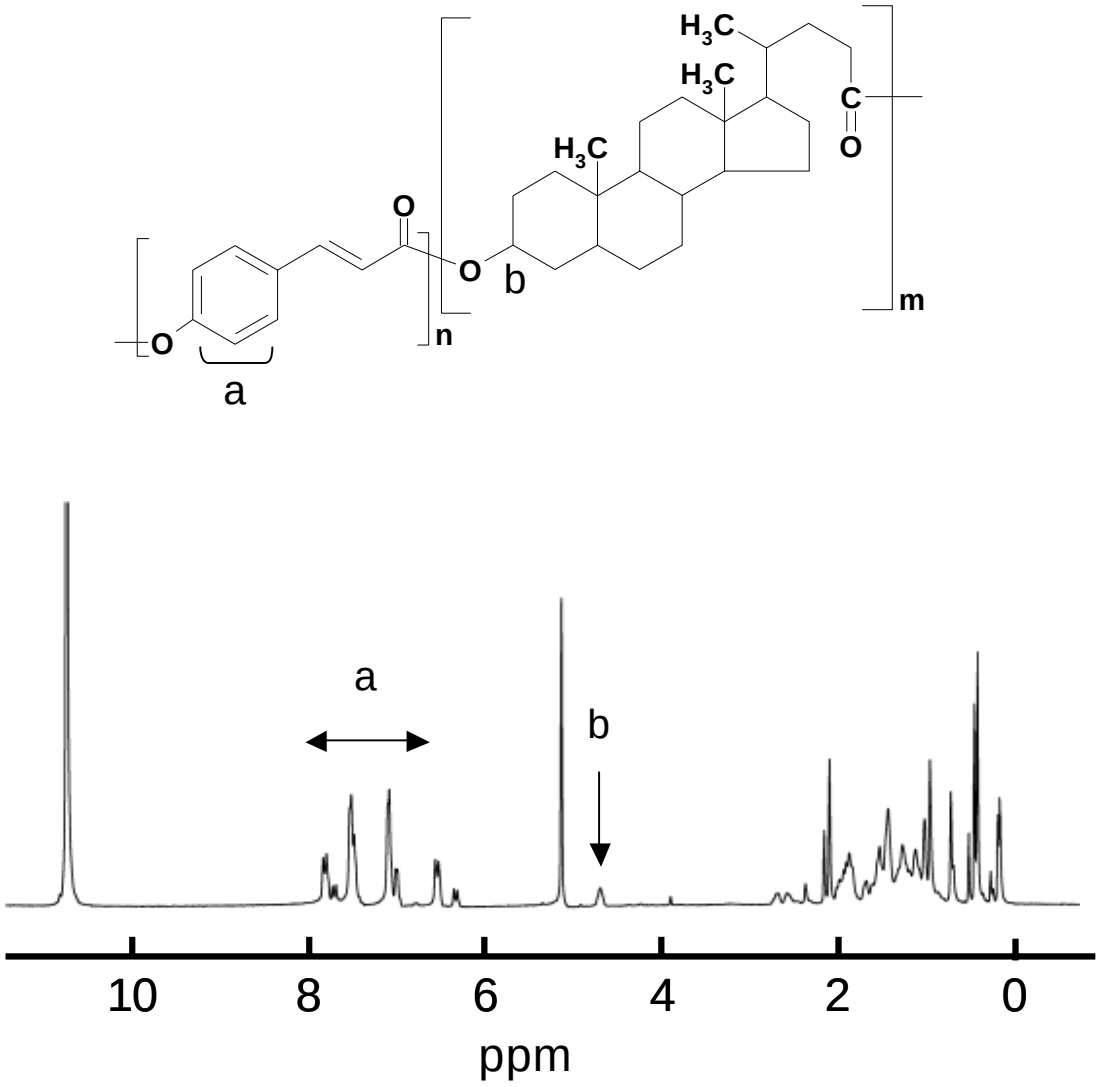


**Figure 2** Matsusaki et al.

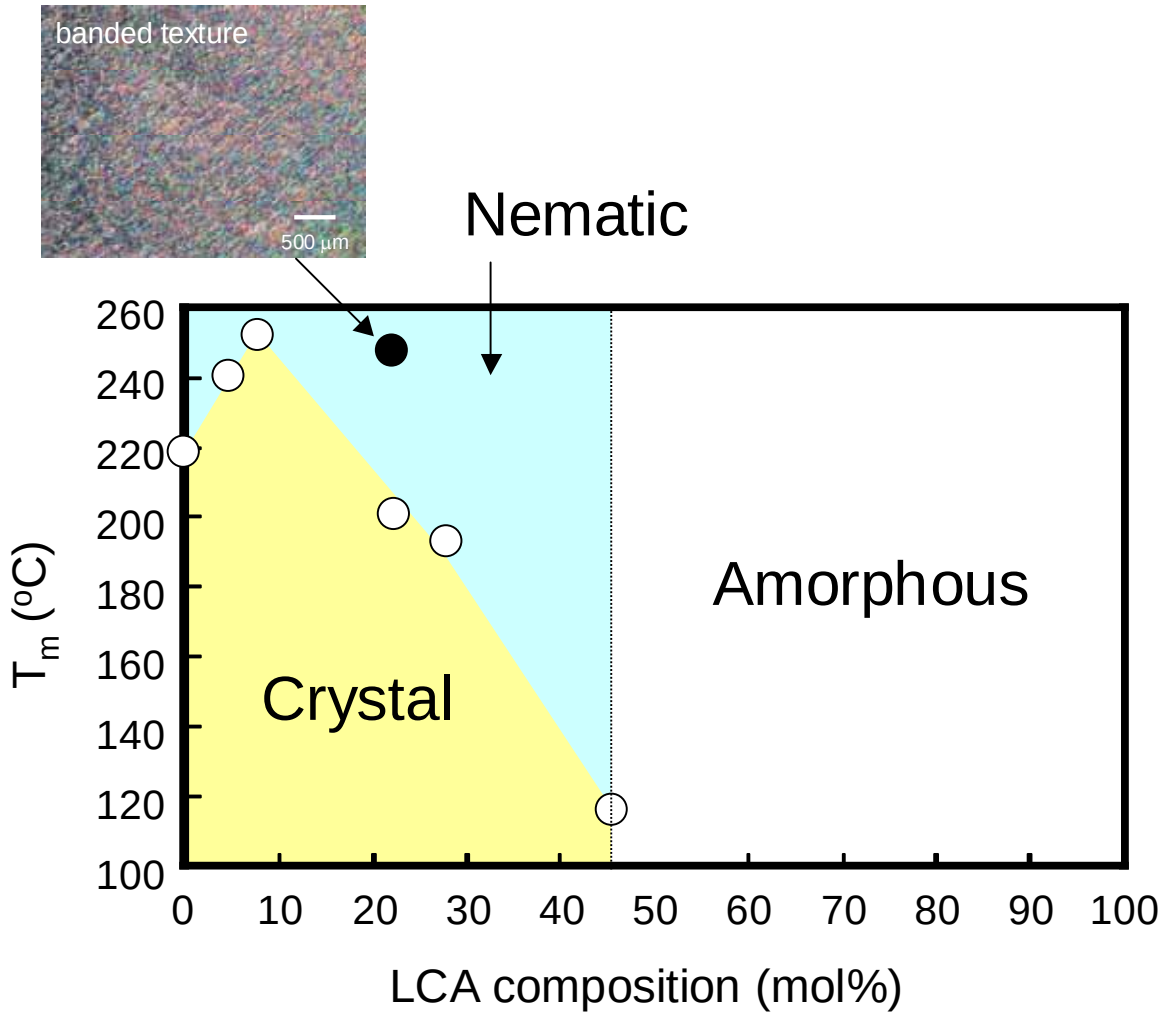


**Figure 3** Matsusaki et al.

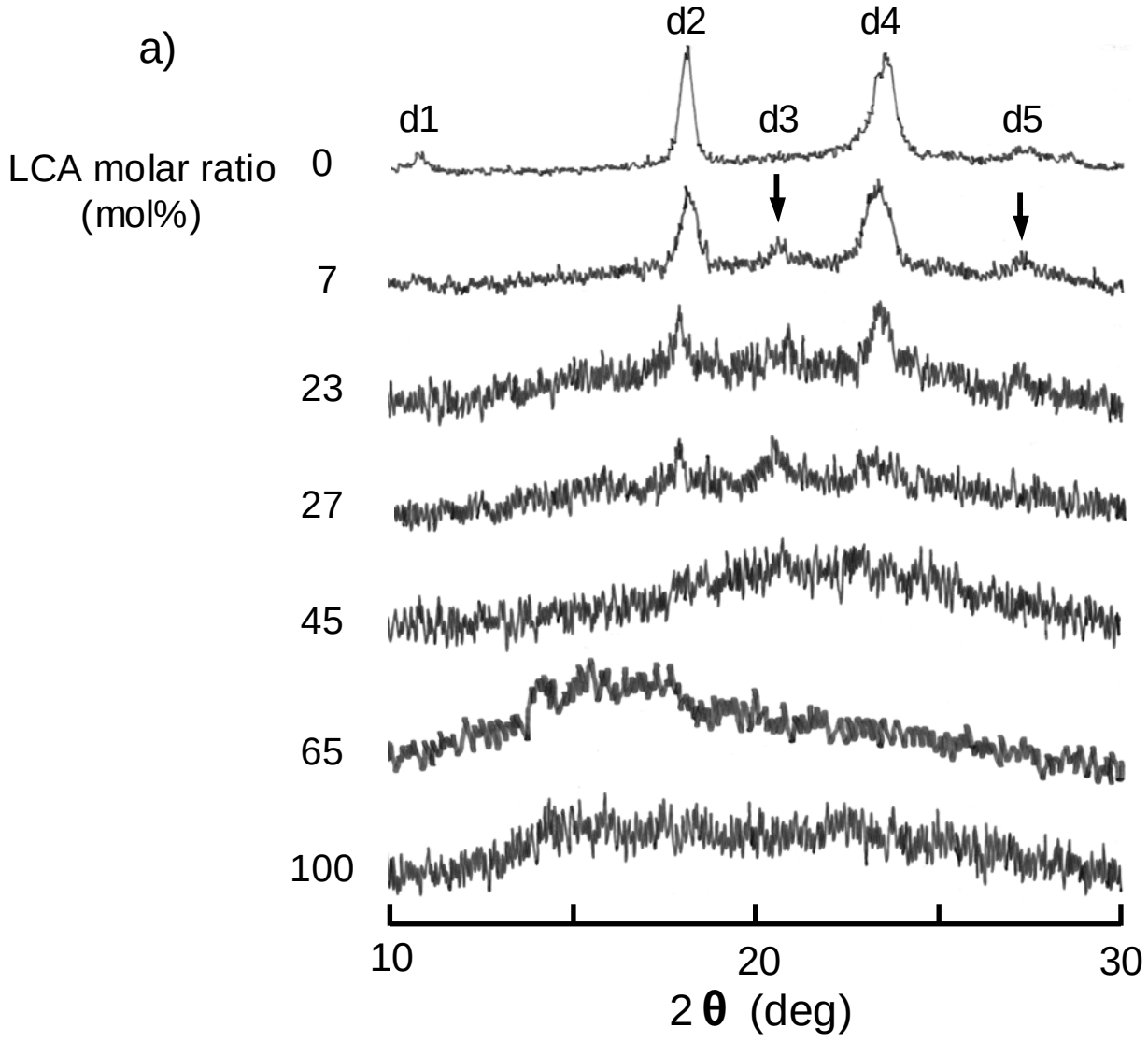


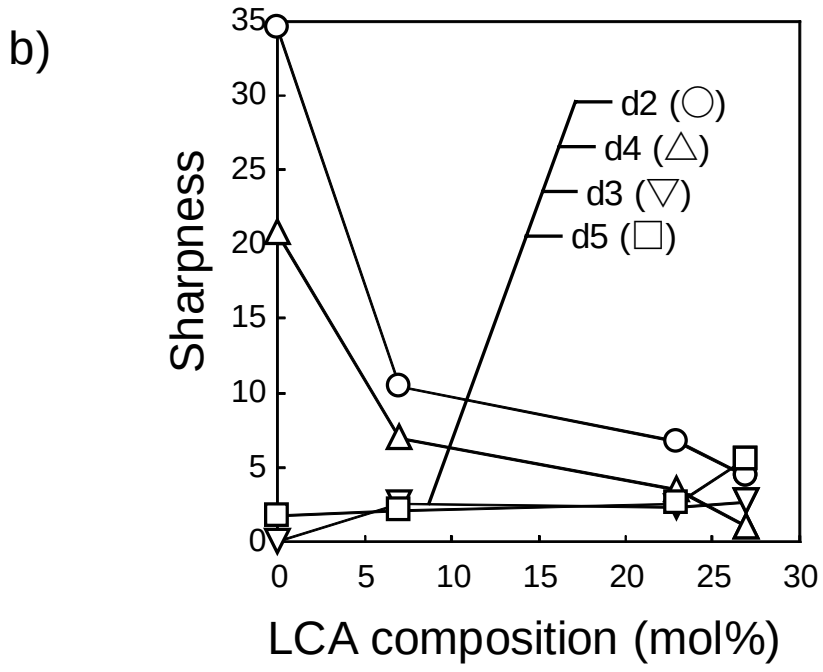


**Figure 4** Matsusaki et al.

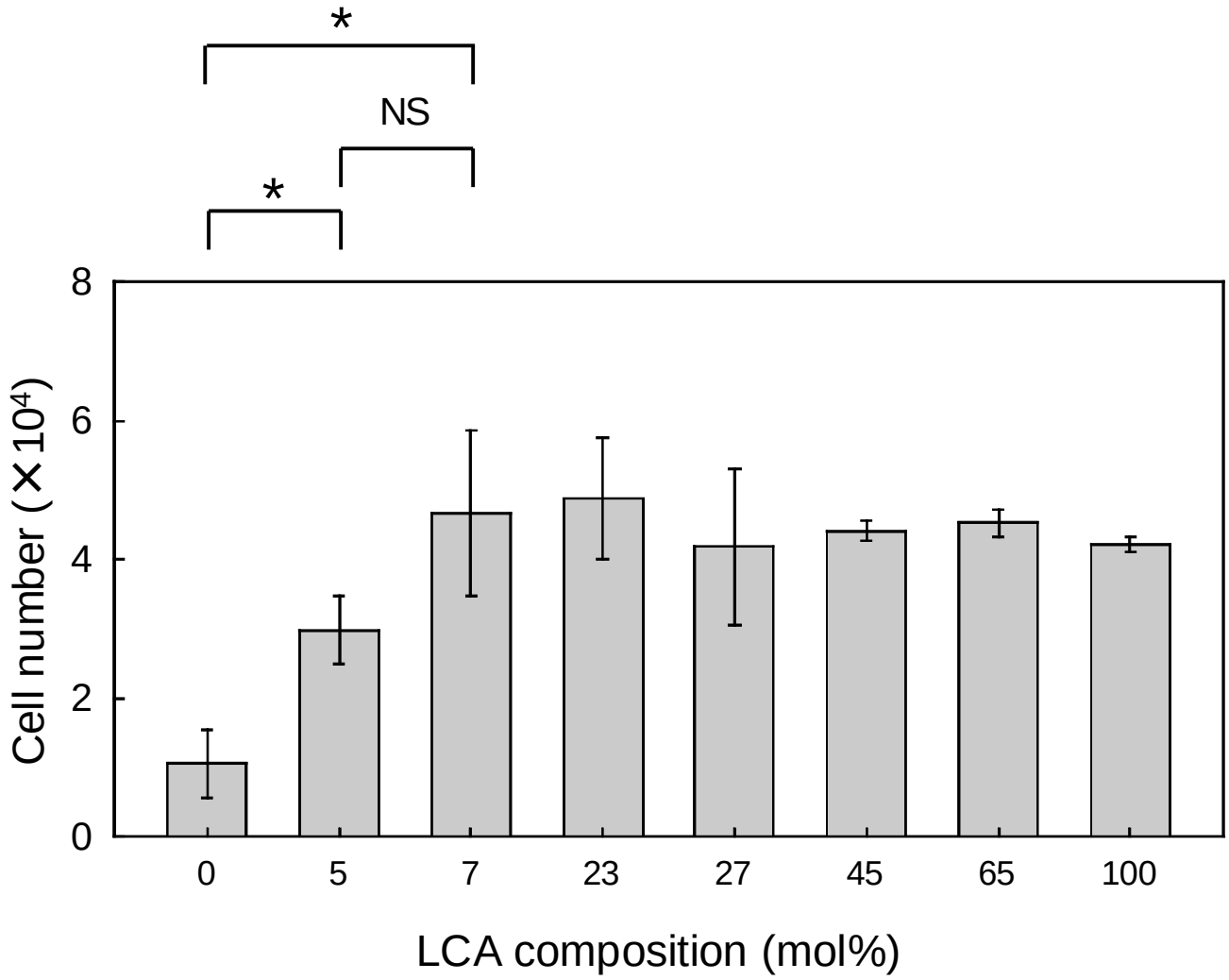


**Figure 5** Matsusaki et al.

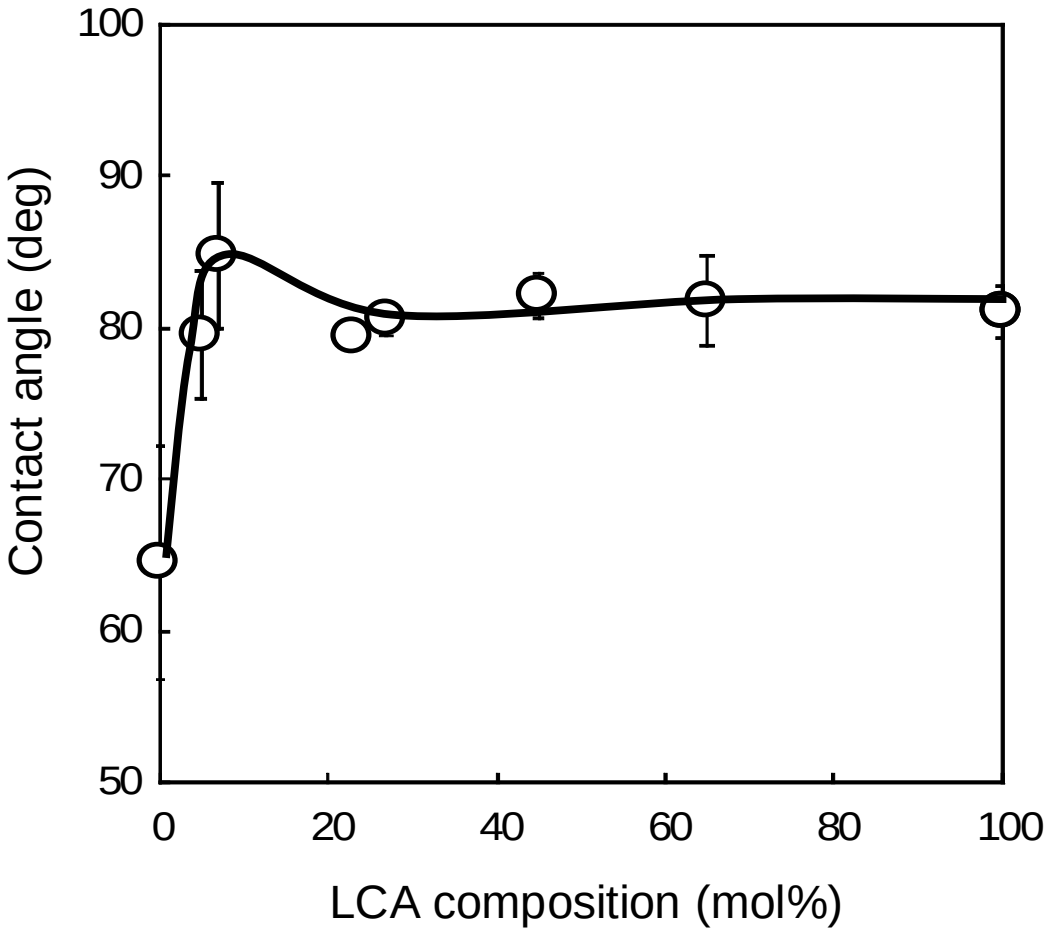


**Figure 6** Matsusaki et al.